Adaptive controller for PMSG wind turbine systems with back-to-back PWM converters

Omar Aguilar, Ruben Tapia, Juan M. Ramirez, Antonio Valderrabano

Abstract—**This paper presents an adaptive control strategy for wind energy conversion systems. The control scheme uses a B-spline artificial neural network for tuning controllers when the system is subjected to disturbances. Voltage-source converter is controlled in a synchronous orthogonal d-q frame by an adaptive PI controller. The B-spline neural network must be able to enhance the system performance through online updating parameters. Thus, the paper proposes the use of adaptive PI controllers to regulate the current, frequency, and DC link voltage. MatLab is employed for simulation studies to verify the performance of the proposed strategy.**

I. Introduction

The sudden increase in the price of oil stimulated a number of substantial, government funded programs of research, development and demonstration. Mainly, in recent years the development of wind energy conversion systems (WECS) has been increased. The expansion of WECS in some countries has been more rapid than in others, and this variance cannot be explained simply by differences in the wind speeds [1].

Nowadays, doubly fed induction generators (DFIGs) are widely used as the generator in a variable speed wind turbine system. The DFIG needs a gearbox to match the turbine and rotor speed. The variable speed wind turbine reliability can be improved significantly using a direct drive-based permanent magnet synchronous generator (PMSG). The PMSG has the following main characteristics: (i) full operating speed range; (ii) brushless; (iii) full scale power electronic converter; (iv) complete control of active and reactive power exchanged with the grid [2]. Power electronics, being the technology of efficiently converting electric power, plays an important role in wind power systems. It is an essential element for integrating the variable speed wind power units to achieve high efficiency and high performance in power systems. Even in a fixed speed wind turbine, where wind power generators are directly connected to the grid, thyristors are used as soft-starters. In particular, voltage sourced converter (VSC) units are used to match the characteristics of wind turbines with the requirements of grid connections, including frequency, voltage, control of active and reactive power, harmonics, etc. [3].

For a grid connected distributed generation unit, the interface is conventionally controlled as a current controlled VSC (CC-VSC). Thus, the VSC's direct-quadrature current components are used to provide instantaneous control of active and reactive power exchange between the VSC and the grid [4]. In this context, a decoupled instantaneous active and reactive power control capability has been demonstrated in [5]-[6]. However, the non-linear nature and wide range of the VSC's operation requirements impose considerable difficulty in control design. Four-quadrant power control requires the power converter AC output voltage and/or current amplitude to vary within the full-rated range and phase angle, while the control variables are all related to DC voltage [7].

Major techniques to regulate the CC-VSC output current include either a variable switching frequency, such as the hysteresis control scheme, or fixed switching frequency schemes, such as the ramp comparison, stationary, and synchronous frame proportional–integral (PI), optimal, nonlinear, adaptive and robust, predictive control, and soft computing or control techniques such as fuzzy control, neural networks control, and on the fusion or hybrid of hard and soft control techniques [8].

When a conventional PI control is used, the parameters have to be tuned, and since it is a linear technique and the parameters are fixed, the good performance of the system can only be assured around the operating point for which the parameters were adjusted. On the other hand, using the parameters from PI scheme like input for an adaptive technique, some author mixed neural networks and PID techniques to strengthen the linear controller. In [9], [10] a back propagation neural networks was used to adjust coefficients k_p, k_i, and k_d of PID controllers attaining power regulation of wind turbines. The similar PID tuning strategy using radial basis function (RBF) neural network for pitch angle control systems [11]. However, tuning alternatives are needed for electrical grid complexity. In these work we proposed a good adaptive tuning technique based on B-spline neural network (BSNN).

The objective is to adaptively adjust the gains in accordance to the present grid operating condition. This is achieved by a strategy to update conventional PIs currently operating in electrical grid that were tuned time ago. The main idea is to re-tune basically the PIs gains through an on-line procedure, which involve a few measurements.

Usually, the VSC synchronization is made by a phase-locked

Manuscript received March 8, 2013. This work was supported in part by the FOMIX-CONCAYT under Grant 130107 and PROMEP Redes Temáticas de Colaboración.

O. Aguilar and R. Tapia are with the Engineering Department, Universidad Politécnica de Tulancingo, Calle Ingenierías 100, Huapalcalco, Hidalgo, México (phone: 775-755-8326, e-mail: ruben.tapia,[omar.aguilar]@upt.edu.mx).

J. M. Ramirez is with the Electrical Engineering Department, CINVESTAV, Av. del Bosque 1145, colonia el Bajío, Zapopan, 45019, Jalisco, México (e-mail: jramirez@gdl.cinvestav.mx).

A. Valderrabano is with the Mechatronics Department, Universidad Panamericana Campus Guadalajara, Calzada Circunvalación Poniente #49 Ciudad Granja CP 45010 Zapopan, Jalisco, México (e-mail: antonio.valderrabano@inbox.com)

978-1-4673-6129-3/13/$31.00 ©2013 IEEE

loop (PLL) system. Nevertheless, having a good synchronization permits a good grid voltage phase and amplitude monitoring, and enhancing the capability of injecting power into the grid. A good PLL design may provide further advanced functionalities to the control system, as it is the case for the islanding detection mode for wind farms [12].

II. WIND ENERGY CONVERSION SYSTEM

A WECS is a structure that transforms the kinetic energy from the wind into electrical energy. This system consists mainly of three parts: (i) a wind turbine drive train; (ii) an electric generator; (iii) a back-to-back converter, Fig. 1 [8].

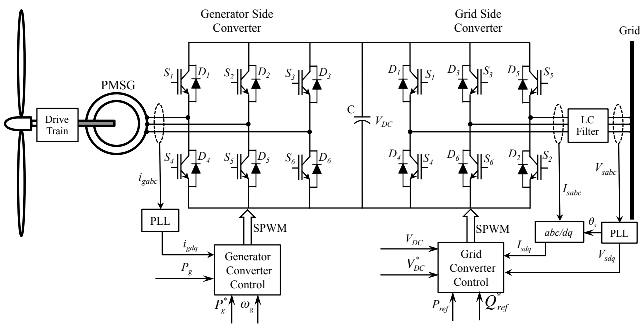

Fig. 1. Wind energy conversion scheme using PMSG.

A. Permanent Magnet Synchronous Generator Model

The PMSG is modeled under the following simplifying assumptions: (i) sinusoidal distribution of stator winding; (ii) electric and magnetic symmetry; (iii) negligible iron losses and unsaturated magnetic circuit. The PMSM's voltage and electromagnetic torque equations in the d-q reference frames are given by the following equations [13]:

$$v_d = -R_s i_d - L_d \frac{di_d}{dt} + L_q i_q \omega_s \quad (1)$$

$$v_q = -R_s i_q - L_q \frac{di_q}{dt} + \left(L_d i_d - \psi_m\right)\omega_s \quad (2)$$

where v_d, v_q, i_d and i_q are the d-q axis voltages and currents, respectively; R_s is the stator resistance; L_d and L_q are the d-q axis inductances; ω_s is the generator rotational speed; ψ_m is the permanent magnetic flux. Under the steady state condition derivative terms are zero,

$$v_d = -R_s i_d + L_q i_q \omega_s \quad (3)$$

$$v_q = -R_s i_q + \left(L_d i_d - \psi_m\right)\omega_s \quad (4)$$

Normally, the difference between the d-q axis mutual inductance is very small for a direct-driven multi-pole PMSG, and the stator winding resistance is much smaller than the synchronous reactance. Therefore $T_e = \mathrm{p} i_q \psi_m$; p is the number of pole pairs.

B. Wind Turbine Model

The mechanical power extracted by a wind turbine is expressed by the cube law equation [13],

$$P_{wt} = 0.5\rho\pi R^2 \mathrm{v}^3 C_p(\lambda) \quad (5)$$

where ρ is the air density; R is the blade length; ω_l is the rotor speed; v is the wind speed and; $C_p(\lambda)$ is the turbine performance coefficient. C_p is a function of the tip-speed-ratio λ. Using generator convention; the rotational speed of the generator and wind turbine driving torque becomes [13],

$$J\frac{d\omega_h}{dt} = \Gamma_{wt} - T_e - B\omega_h \quad (6)$$

$$T_e = p\left[\psi_m i_q + \left(L_d - L_q\right) i_d i_q\right] \quad (7)$$

where Γ_{wt} is the turbine driving torque referred to the generator ($\Gamma_{wt} = P_{wt}/\omega_l$); B is the active damping coefficient representing turbine rotational losses; and $\omega_h = i\omega_l$, where i is the ratio of a rigid drive train.

III. BACK TO BACK CONVERTER MODEL

Fig. 1 illustrates that back-to-back converter system can be considered as the composition of two VSC: the right-hand side includes the DC-voltage, active and reactive power controllers, and the left-hand side controls the generator's speed. As Fig. 1 shows, the active and reactive power controller and the controlled DC-voltage are interfaced with the PMSG and the grid, respectively. WECSs are requested to operate robustly in different grid locations and to keep ancillary services in order to behave as a conventional power plant. The control scheme for the WECS-based on PMSG is designed to satisfy grid requirements.

The diagram of a three-phase three-wire VSC connected to the AC system, represented by an equivalent Thevenin circuit via the inductance and resistance (L_T, R_T) of the coupling transformer is presented in Fig. 1. The converter's DC terminal is connected to a shunt capacitance (C_{dc}) and resistance (R_{dc}), which represent switching losses. The DC and AC side power balancing are expressed as [7]:

$$\frac{d\mathbf{I}_{abc}}{dt} = \frac{1}{L_s + L_T}\left[-\left(\mathbf{R}_s + \mathbf{R}_T\right)\mathbf{I}_{abc} + \mathbf{V}_{Sabc} - \mathbf{V}_T\right] \quad (8)$$

$$\frac{dV_{dc}}{dt} = \frac{1}{C_{dc}}\left[-\frac{V_{dc}}{R_{dc}} + \mathbf{I}_{abc}^T \frac{\mathbf{V}_T}{R_{dc}}\right] \quad (9)$$

Using the orthogonal transformation, it can be,

$$\frac{dI_d}{dt} = -aI_d + \omega I_q + bV_{sd} - bV_{Td} \quad (10)$$

$$\frac{dI_q}{dt} = -\omega I_d - aI_q + bV_{sq} - bV_{Tq} \quad (11)$$

$$\frac{dV_{dc}}{dt} = \frac{1}{C_{dc}}\left[-\frac{V_{dc}}{R_{dc}} + \frac{1}{V_{dc}}\left(i_d v_{Td} + i_q v_{Tq}\right)\right] \quad (12)$$

where $a = (R_s + R_T)/(L_s + L_T)$, $b = 1/(L_s + L_T)$.

In some applications the Park transformation is not employed but its inverse is necessary; it depends on the control design. That is, the inverse Park transform allows, from constant values generating signals in-phase or anti-phase, respect to the reference. That is especially useful for flexible AC transmission systems (FACTS) and power conditioners' control [14]. Instantaneous complex power are expressed by [14], [15],

$$S = \left(V_{Td}I_{Td} + V_{Tq}I_{Tq}\right) - j\left(V_{Tq}I_{Td} - V_{Td}I_{Tq}\right) \tag{13}$$

Equation (13) suggest that if $V_{Tq} = 0$, the active and reactive power components are proportional to i_d and i_q, respectively. This property is widely employed in the control of grid-connected three-phase VSC systems [15]. The angle θ of the grid voltage is computed and provided by a phase-locked loop. The PLL is responsible for measuring the angle of the reference vector respect to the axis α. Therefore, it is possible to assess the direct or reverse Park transformation. There exist a variety of PLL structures. The evaluation of the $tan^{-1}(\beta/\alpha)$ is an easy way to estimate, taking care of the signals' sign [12], [15]-[16].

IV. CONTROL WECS-BASED ON PMSG

The main advantage of the back-to-back converter is that it allows independently handle the active and reactive power flow between two AC systems with different characteristics (fundamental frequency, switching frequency, input voltage, etc.), However, to achieve this, it is necessary to investigate control strategies to attain the desired values. In the control scheme, the generator side's converter controls the rotor speed for maximum power extraction, using a feedforward control to produce the control signals in dq-frame. Thus, we have two decoupled, first order linear systems, Fig. 2. The grid side's converter regulates the DC-link voltage, and also the reactive power flow between the wind generator and the grid. Due to their simplicity, schemes based on classical PI controllers used in the d-q frame are implemented for controlling DC voltage.

A. Generator side converter control

The generator side control scheme is shown in Fig. 2. There are two PI controllers used in the strategy. The generator side three-phase converter uses a PI control strategy and works as a driver controlling the generator operating at optimum rotor speed ω_{opt} to obtain maximum energy from wind [13]. ω_{opt} is approximated as $\omega_{opt} = 0.1874v$, [17] This represent the desired value of the shaft speed, for maximum power extraction [13].

The inner loops are constituted by two controllers, which regulate the d and q-axis of the stator currents. The electromagnetic torque may be controlled directly by the q-axis current component i_q, therefore the speed can be controlled by changing q axis current, and d-axis current component i_d is set to zero to minimize the current and resistive losses for a given torque. The outputs from the two current controllers are the d and q-axis stator voltage references, which are sent to the sinusoidal pulse-width modulation (SPWM) block. The SPWM will generate the switching signals required by the IGBT elements of the converter.

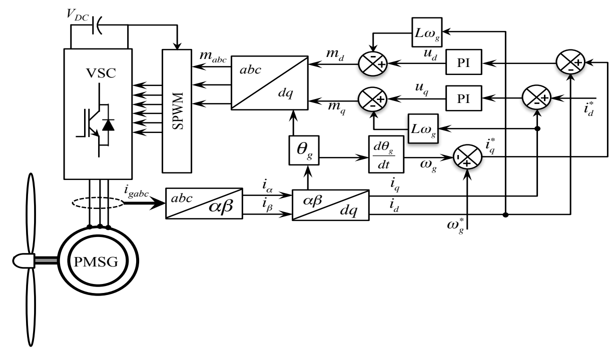

Fig. 2. Block diagram of generator side converter control scheme.

B. Grid side converter control

The control scheme of this strategy is exhibited in Fig. 3. The main task of the grid side converter control is to supply a reliable electric power to the consumers, regulating converter output variables such as voltage and frequency. Another function of controller is the constancy of the DC-link voltage (DCLV), while controlling the active and reactive power. This action is attained through the phase angle and the amplitude of the VSC's line current i_d and i_q. The feedback and feed-forward signals are first transformed to the d-q frame and then processed by compensators to produce the control signals. These control signals are transformed to the abc-frame and sent to the grid side converter.

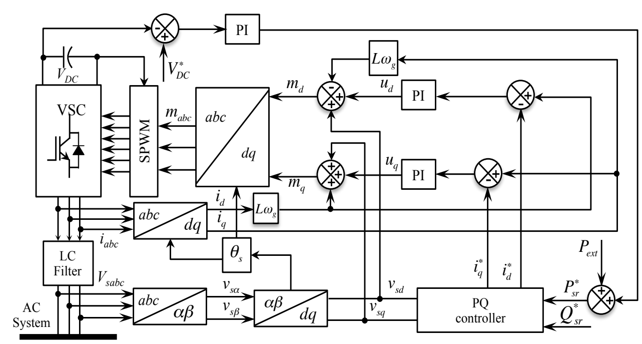

Fig. 3. Block diagram of grid side converter control.

The active power reference, P_{g_ref}, may be determined by examining the DC link dynamics. The power balance at the DC link is [18],

$$P_c = P_g - P_n \tag{14}$$

where P_c is the power that goes through the DC link capacitor; P_g is the generator's active power output; and P_n

is the active power transmitted from the DC link to the grid. The DCLV, V_{dc}, is determined as follows:

$$\frac{dV_{dc}^2}{dt} = \frac{2}{C} P_c \tag{15}$$

The active power reference, P_{n_ref}, is calculated by comparing the actual DCLV, with respect to the desired DCLV reference, V_{dc_ref}. This error is processed by a control scheme, the output becomes P_{n_ref}.

V. Neural Controller Topology

The proposed can be achieved adding a B-spline neural network to update all gains in five PI controllers, generator and grid side. Each PI transfer function is given by

$$\frac{U(s)}{E(s)} = \frac{k_i}{s} + k_p \tag{16}$$

Thus, k_p and k_i are updated from a B-spline neural network at every sampled time. With this purpose, ten BSNN are assembled in the control scheme.

A. B-spline neural network

B-spline NN belong to a class of networks known as lattice-based Associative Memory Networks (AMN), used generally for functional approximation tasks. The network has a fixed structure and a set of adaptive parameters that are iteratively trained in order to achieve the desired behavior, with the option of carrying out such tasks on-line, and taking into account the power grid non-linearities. The on-line B-spline associative memory network (AMN) adjusts its weights iteratively in an attempt to reproduce a particular function, whereas an off-line or batch B-spline algorithm typically generates the coefficients by matrix inversion or using conjugate gradient. B-spline AMNs adjust their (linear) weight vector, generally using instantaneous least mean square (LMS)-type algorithms, in order to realize a particular mapping, modifying the strength with which a particular basis function contributes to the network output. Through BSNN there is the possibility to bound the input space by the basis functions definition.

The BSNN's output can be described by [19],

$$\begin{gathered} y = \mathbf{a}^T \mathbf{w} \\ \mathbf{w} = \begin{bmatrix} w_1 & w_2 & \dots & w_n \end{bmatrix}^T; \quad \mathbf{a} = \begin{bmatrix} a_1 & a_2 & \dots & a_n \end{bmatrix}^T; \end{gathered} \tag{17}$$

where w_i and a_i are the i-th weight and the i-th BSNN basis function output, respectively; n is the number of weighting factors. i refers to sub index that can take values from 1 to n (vector dimension); and n represents the number of weighting factors, it depends on a particular application. In this case, only two weight's factor was used to each ANN, Fig. 4. It allows diminish the computational effort with well system response. In this paper it is proposed that k_p and k_i be adapted through one BSNN, respectively, for each voltage source converter. The error signals are the same of PI controllers. Then the dynamic control parameters for back to back system can be described as follows:

$$k_x = NN_m\left(e_x, w_i\right) \tag{18}$$

where NN_m denotes the BSNN which is used to calculate k_p and k_i; w_i is the corresponding weighting factor; m=1,2,3 number of PI controllers. Fig. 4 depicts a scheme of the proposed BSNN.

The appropriate design requires the following a-priori information: the bounded values of e_x, the size, shape, and overlap definition of the basis function. Likewise, with this information the BSNN estimates the optimal weights' value. The neural network adaptive parameters, (17)-(18) are created by univariate basis functions of order 3, considering that e_x is bounded within [-1.5, 1.5].

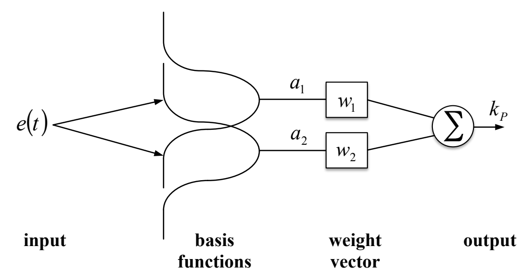

Fig. 4. Proposed BSNN for adapting k_p and k_I control parameters.

B. B-spline learning

Many neural network training rules are simply instantaneous algorithms (together with nonlinear variations) and in recent years there has been a growing interest in trying to understand what and how neural networks learn. The learning must be local, in that the parameters adapted should only affect the output of the network locally. Instantaneous learning rules are formulated by minimizing instantaneous estimates of a performance function, which is generally the Mean Square output Error (MSE), and the parameters are updated using gradient descent rules. The B-spline network depends linearly on a set of weights, and they are these parameters, which are updated using the basic learning rules.

On-line learning of continuous functions, mostly via gradient-based methods on a differentiable error measure is one of the most powerful and commonly used approaches to train large layered networks in general [20], and for nonstationary tasks in particular. In this application, the parameters' quick updating is looked for. While conventional adaptive techniques are suitable to represent objects with slowly changing parameters, they can hardly handle complex systems with multiple operating modes. The instantaneous training rules provide an alternative so that the weights are continually updated and reach the convergence to the optimal values. Also, conventional nets sometimes do not converge, or their training takes too much time [20-21].

In this paper, the BSNN is trained on-line using the following error correction instantaneous learning rule [19],

$$w_i = w_i(t-1) + \frac{\eta e_i(t)}{\|\mathbf{a}(t)\|_2^2} a_i(t) \tag{19}$$

where η is the learning rate and e_i (t) is the instantaneous output error.

Respect to the learning rate, it takes as initial value one point within the interval [0, 1] due to stability purposes. This value is adjusted by trial-and-error. If η is set close to 0, the training becomes slow. On the contrary, if it is large, oscillations may occur. In this application, it settles down in 0.051 for k_p, and 0.0016 for k_i. The BSNN training process is carried out continuously on-line, while the weights' values are updated.

It is proposed that during the actualization procedure, a dead band is included to improve the learning rule convergence. The weighting factors are not updated if the error has a value below 0.1%,

$$w_i(t) = \begin{cases} w_i(t-1) + \dfrac{\eta e_i(t)}{\|\mathbf{a}(t)\|_2^2} a_i(t), & \text{if } |e_i| > 0.0001 \\ w_i(t-1), & \text{otherwise} \end{cases} \tag{20}$$

This learning rule has been elected as an alternative to those that use, for instance, Newton's algorithms for updating the weights that require Hessian and Jacobian matrix evaluation. Regarding the weights' updating, (20) should be applied for each input-output pair in each sample time; the updating occurs if the error is different from zero.

The parameters are chosen by trial-and-error, following the heuristic given in [19], which states that the simplest acceptable adaptive system produces the best results. The position of the knots is selected using a priori information about the system. The learning rate values are elected based on a compromise between fast learning and greater noise filtering.

VI. Test Results and Analysis

In order to demonstrate the feasibility of this proposition, a wind generation system is employed. Matlab are used for simulation. To analyze the results, simulations are developed under different scenarios with PI controllers tuned by BSNN (dynamic parameters). Some operating conditions are taken into account. The models of the medium-power (2.5 kW) rigid drive train PMSG based WECS shown in Fig. 1 are included in the simulations.

Major system parameters are listed in Table I [13]. The power converter and the control algorithm are also implemented and included in the model. The sampling time used for the simulation is 20 µs. It is assumed that wind speed profile varies smoothly with step rate at different slopes, Fig. 5. The system is subjected to the following sequence of events: until t = 0.033 s, $P_{ref} = 2400$ W, $Q_{s\_ref} = 0$. At t = 0.033 s, P_{ref} is subjected to a step change from 2400 to 1800 W. At t = 0.66 s, P_{ref} is subjected to another step change from 1800 to −1500 W and Q_{s_ref} is subjected to step change from 0 to 100 VAR.

Table I
Parameters of PMSG Wind Power System.

Blade length	R = 2.5 m
Multiplier ratio	7
Efficiency	η=1
HSS inertia	J=0.5042 kg m^2
No. of pairs of poles	3
Armature resistance	3.3 Ω
Stator inductance	L_d=L_q=41.56 mH
Magnetic flux Linkage	ψ_m = 0.4382 Wb

Fig. 6 shows the simulation result of DC link voltage with the proposal and considering fixed parameters. Fig. 7 exhibits the dynamic behavior of the reactive power at DC link bus. The transient response is diminished in terms of the overshot without parameters update. The adaptive neural network PI exhibits very well performance adapting itself to the new conditions. Fig. 7 illustrates that P_s and Q_s rapidly track P_{s_ref} and Q_{s_ref}, respectively.

Fig. 8 shows the instantaneous currents under load variations. The load current is changing respect to the load variations as expected. There is no significant rise in the current waveform during the transient. The adaptive controller parameters performance can decrease the oscillations amplitude and transient time under different operating conditions, respect to the behavior with fixed control parameters.

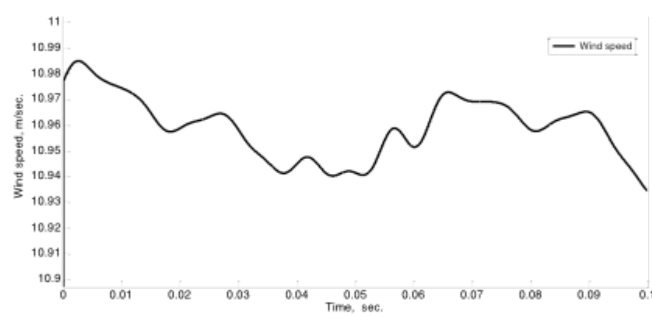

Fig. 5. Wind speed variation.

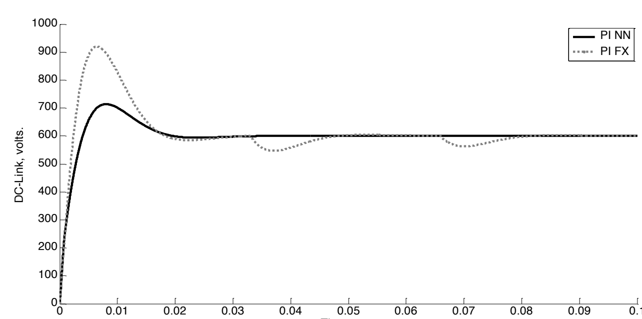

Fig. 6. DC link voltage performance.

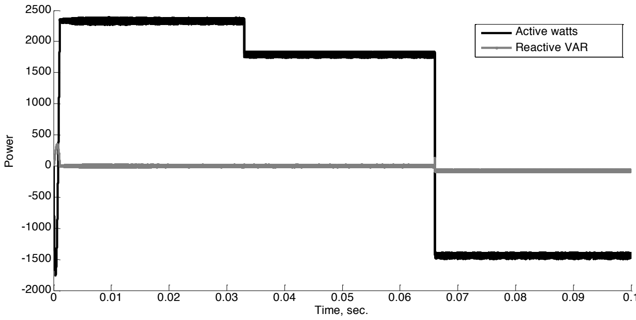

Fig. 7. Active and reactive power in WECS terminals.

The aim of the paper is to show the performance of adaptive PI parameters as a mean to enhance VSC performance. In order to attain such purposes a BSNN is proposed. With this neural adaptive scheme, the possibility to implement the on-line updating parameters is potential due to it has learning ability and adaptability.

Unlike the conventional technique, the BSNN exhibits an adaptive behavior since the weights can be adapted on-line responding to inputs and error values as they arise.

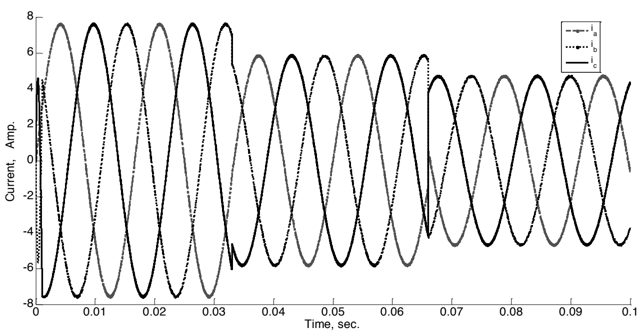

Fig. 8. Instantaneous output line current.

VII. Conclusion

The aim of this paper is to show the performance of adaptive PI parameters as a mean to tune linear controllers in WECS system. In order to attain such purposes a B-spline neural network-based is proposed. With this neural adaptive scheme, the possibility to implement the on-line updating parameters is potential due to it has learning ability and adaptability, robustness, simple algorithm and fast calculations This is desirable for practical hardware implementation in power stations.

References

[1] T. Burton, N. Jenkins, D. Sharpe and E. Bossanyi, *Wind Energy Handbook*, 2nd ed., United Kingdom: Wiley, 2011, pp. 1-8.

[2] G. Abad, J. López, M. A. Rodríguez, L. Marroyo and G. Iwanski, *Doubly Fed Induction Machine*, New Jersey: Wiley, 2011, pp. 1-25.

[3] J. Yao and D. Popovic, "Stability of a MV distribution network with electronically interfaced distributed generation," in *Proc. 2004 IEEE Mediterranean Electrotechnical Conf.,* pp. 975–978.

[4] Z. Chen, J. Guerrero, and F. Blaabjerg, "A Review of the State of the Art of Power Electronics for Wind Turbines," *IEEE Trans. on Power Electronics,* vol. 24, pp. 1859-1875, Aug. 2009.

[5] F. Gao, and M. Iravani, "A Control Strategy for a Distributed Generation Unit in Grid-Connected and Autonomous Modes of Operation", *IEE Trans. Power Delivery,* Vol. 23, pp. 850-859. April 2008.

[6] N. Hingorani and L. Gyugyi, *Understanding FACTS: Concepts and Technology of Flexible AC Transmission Systems*, New York: Wiley, 1999.

[7] J. Arrillaga, Y. Liu, N. Watson and N. Murray, *Self-Commutating Converters for High Power Applications*, United Kingdom: Wiley, 2009.

[8] K. Dai, P. Liu, Y. Kang, and J. Chen, "Decoupling current control for voltage source converter in synchronous rotating frame," presented at the 4th Int. Conf. *IEEE Power Electronics Drive Systems*, Bali, Indonesia, 2001.

[9] X. Yao, X. Su, and L. Tian, "Wind turbine control strategy at lower wind velocity based on neural network PID control," *in Intelligent Systems and Applications, 2009. ISA 2009. International Workshop on*, May. 2009.

[10] Z. Xing, Q. Li, X. Su, and H. Guo, "Application of BP neural network for wind turbines," *in Intelligent Computation Technology and Automation, 2009. ICICTA '09, Second International Conference on*, vol. 1, Oct. 2009.

[11] X. Yao, X. Su, and L. Tian, "Pitch angle control of variable pitch wind turbines based on neural network PID," *in Industrial Electronics and Applications, 2009. ICIEA 2009. 4th IEEE Conference on*, May. 2009.

[12] A. Luna, J. Rocabert, G. Vazquez, P. Rodríguez, R. Teodorescu and F. Corcoles, "Grid Synchronization for Advanced Power Processing and FACTS in Wind Power Systems", in *Proc. 2010 IEEE Industrial Electronics Conf.,* pp. 2915-2920.

[13] I. Munteanu, A. Iuliana B., N. A. Cutululis, and E. Ceanga, *Optimal control of Wind Energy Systems*, London: Springer, 2008, pp. 29-60.

[14] J. C. Rosas, "Simple Topologies for Power Conditioners and FACT's Controllers," Ph.D. dissertation, Cinvestav, Guadalajara, 2009.

[15] A. Yazdani and R. Iravani, *Voltage-Sourced Converters in Power Systems Modeling, Control, and Applications*, New Jersey: Wiley, 2010.

[16] A. Valderrabano and J. M. Ramirez, "Details on the implementation of a conventional StatCom's control," presented at the Int. Conf. *IEEE. Transmission and Distribution: Latin America*, Bogota, Colombia, 2008.

[17] S. Morimoto, H. Nakayama, M. Sanada, and Y. Takeda, "Sensorless output maximization control for variable-speed wind generation system using IPMSG," IEEE Trans. Ind. Appl., vol. 41, no. 1, pp. 60–67, Jan./Feb. 2005.

[18] O. Anaya-Lara, N. Jenkins, J. Ekanayake, P. Cartwright and M. Hughes, *Wind Energy Generation Modelling and Control*, United Kingdom: Wiley, 2009, pp. 110-112.

[19] M. Brown, and C. Harris, *Neurofuzzy Adaptive Modeling and Control*, New York: Prentice Hall, 1994.

[20] D. Saad, "On-line learning in neural networks," Cambridge University Press, 1998.

[21] A. Osman, T. Abdelazim, and O. Malik, Transmission Line Distance Relaying Using on-line Trained Neural Network. IEEE Trans. Power Delivery, vol. 20, No. 2, pp. 1257-1264, 2005.